



51 solution average. The *de facto* method for validating an NMR structure is to compare  
52 it to a crystal structure. Surveys carried out based on such comparisons have shown  
53 that NMR structures are similar to crystal structures, but in general less well defined  
54 (less precise) and also less accurate<sup>6,7</sup>. However, if there are genuine differences  
55 between crystal structures and solution structures (for example due to increased  
56 flexibility in solution and at higher temperatures), then such comparisons will be  
57 misleading. We recently developed a method ANSURR, Accuracy of NMR Structures  
58 Using RCI and Rigidity, which calculates the local rigidity of a protein structure<sup>8</sup>, and  
59 compares it to the local rigidity as measured using a version of the Random Coil Index<sup>9</sup>  
60 based on backbone NMR chemical shifts<sup>10,11</sup>. The method has been tested on a wide  
61 range of structures and provides a reliable guide to accuracy. We have therefore  
62 applied ANSURR to answer the questions posed above.

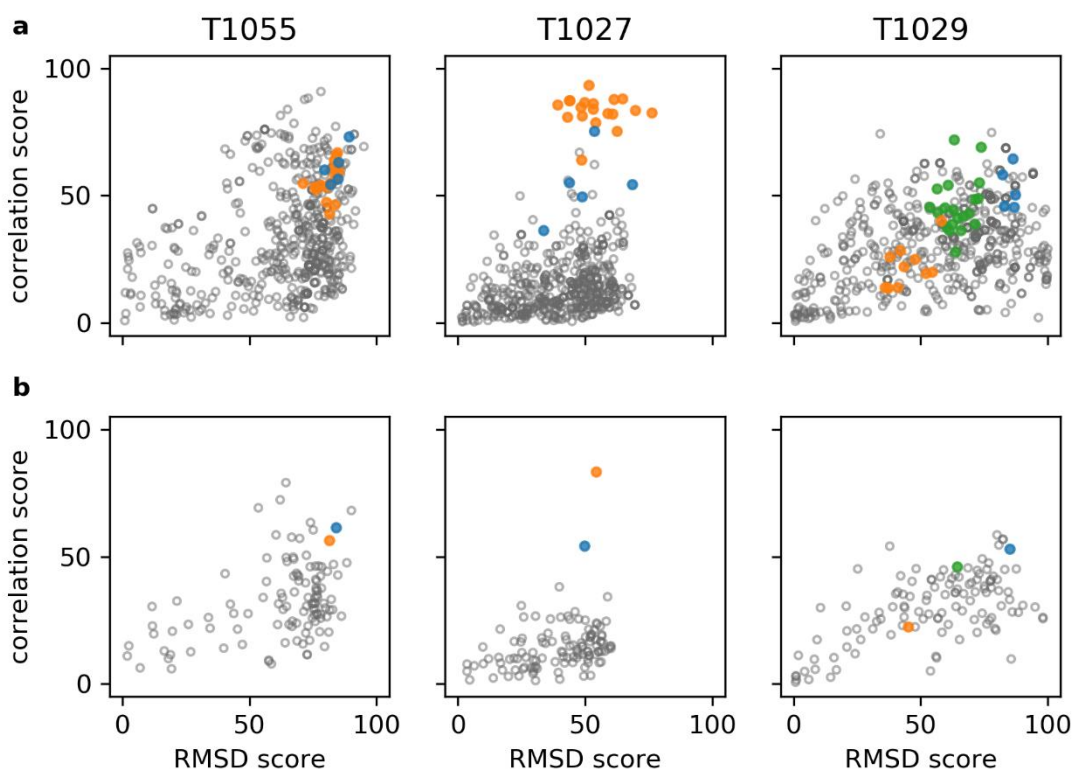
63 The paper is structured as follows. Firstly, we compare the accuracy of three  
64 NMR targets and the corresponding predicted structures from the CASP14  
65 competition, with consideration of both global and local aspects of accuracy. Next, we  
66 expand our study to compare 904 structures of human proteins from the AlphaFold  
67 Protein Structure Database<sup>12</sup> with NMR structures from the Protein Data Bank (PDB),  
68 highlighting instances where NMR structures are significantly more accurate than AF2  
69 models and *vice versa*. Finally, we investigate the relationship between the estimated  
70 accuracy of AF2 models (as predicted by AF2 alongside a structure) with the accuracy  
71 determined by ANSURR.

72  
73

## 74 Results

75

76 **The accuracy of target NMR structures and predicted structures from CASP14.**  
77 ANSURR works by computing two measures of protein flexibility; one obtained from  
78 backbone chemical shifts and the other from a structure using the mathematical theory  
79 of rigidity. The two measures are compared by computing the rank Spearman  
80 correlation coefficient and root-mean-squared deviation (RMSD) between them. The  
81 percentile of each value relative to those for all NMR structures in the PDB is used to  
82 obtain two scores, termed correlation score and RMSD score, respectively. These  
83 scores can be visualised on a single plot so that the best scoring structures (with good  
84 correlation and RMSD scores) appear in the top right-hand corner of the plot and the  
85 worst scoring appear in the lower left-hand corner (with poor correlation and RMSD  
86 scores). CASP14 had three NMR ensembles that were used as targets. These are  
87 shown in Figure 1, using either all the structures in the predicted or experimental  
88 ensemble (Fig 1a), or the scores averaged across all members of the ensemble (Fig  
89 1b). ANSURR scores for all NMR and AF2 models are provided in supplementary  
90 information. One of these (T1055) had AF2 CASP14 predictions that were close to the  
91 NMR target structures. However, the other AF2 predictions were very different, with  
92 one being worse than the NMR target (T1027), and one being significantly better  
93 (T1029). These two structures are now examined in more detail.



94  
95

96 **Figure 1.** ANSURR scores for the three CASP14 NMR targets. Results for (a) all  
97 models and (b) ensemble averages are shown. NMR structures are in orange, AF2  
98 models in blue, and all other predictions in grey. The green points shown for T1029  
99 are scores for an NMR ensemble that was recalculated after the CASP14 results were  
100 released, and are discussed below. The NMR structure for T1055 (PDB 6zyc) has 20  
101 models and the NMR structure for T1027 (PDB 7d2o) has 19 models. The original  
102 NMR structure for T1029 (PDB 6uf2) has 10 models and the recalculated structure  
103 (PDB 7n82) has 20 models. Each group competing in CASP14 could provide up to 5  
104 predictions.

105

### 106 **Target T1027**

107 For target T1027, the target NMR ensemble is more accurate than all predicted  
108 structures. However, the AF2 models are the best scoring of the predicted structures,  
109 with one model approaching the accuracy of the NMR ensemble. Thus far, it is a fairly  
110 unremarkable result. However, interesting lessons can be learnt by a more detailed  
111 analysis, particularly of the ill-defined regions.

112 The CASP14 assessment for T1027 was limited to residues with well-defined  
113 atomic positions across all 19 models in the NMR ensemble. In total, four regions were  
114 considered ill-defined and therefore excluded (Figure 2). This is also standard practice  
115 for many NMR protein structure validation programs, which typically only consider  
116 well-defined regions identified by the program CYRANGE<sup>13</sup>. ANSURR validation is  
117 different in that it requires consideration of the entire protein structure, as excluding  
118 residues will lead to nearby regions becoming artificially too flexible.

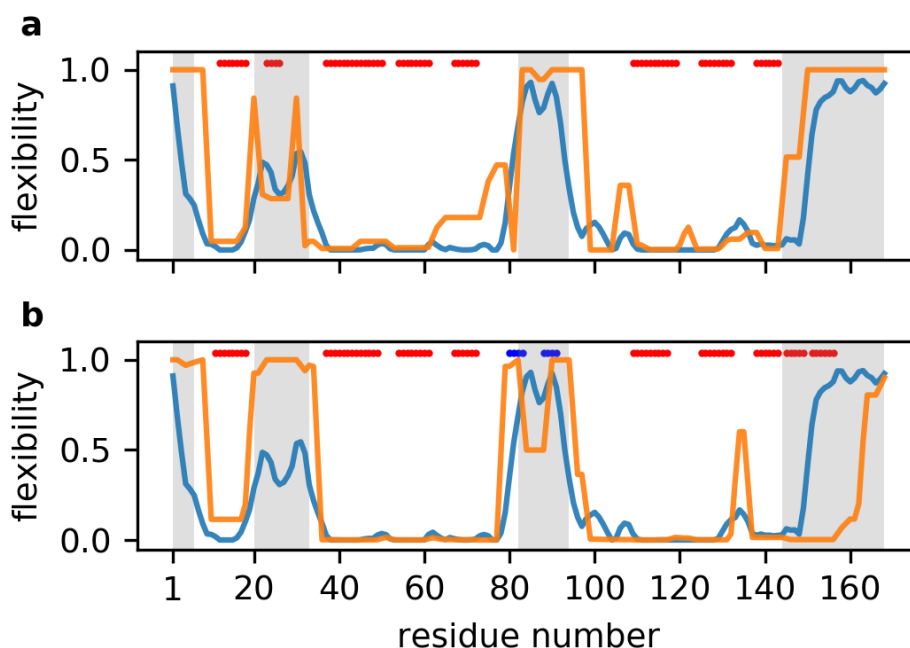
119 The second ill-defined region (Figure 2, residues 20-33) is particularly  
120 interesting. The authors of the NMR structure used  $^{15}\text{N}$  relaxation dispersion and  $^1\text{H}$ -  
121  $^{15}\text{N}$  heteronuclear NOE data to show that this region is dynamic, and suggested it is  
122 intrinsically disordered. However, ANSURR shows it is much less flexible than the  
123 other three ill-defined regions and therefore although it is dynamic, it is not intrinsically  
124 disordered. There is also a noticeable reduction in flexibility in the center of this region.  
125 Both of these features are reflected in the computed flexibility of the NMR structure,  
126 but not in the AF2 structure. The NMR structure has a short  $\alpha$ -helix in this region that  
127 acts to reduce the flexibility of the surrounding area, whereas this region is completely  
128 disordered in the AF2 structure (SI Figure 1a,b). Our ANSURR analysis suggests this  
129 region is flexible, in agreement with dynamic NMR measurements, but is not  
130 intrinsically disordered. ANSURR thus suggests that the helical structure is present in  
131 solution, for the majority of the time.

132 Chemical shifts suggest the third ill-defined region (residues 82-94) is highly  
133 disordered. There is a small reduction in flexibility between residues 86-89. This region  
134 is completely disordered in the NMR ensemble. The slight reduction in computed  
135 flexibility in this region for model 11 (shown in Fig 2a) originates from two weak  
136 hydrogen bonds, but is not observed for any of the other models from the ensemble.  
137 In contrast, the AF2 models comprise a loose  $\beta$ -sheet-like structure linked by a  
138 moderately rigid turn (SI Figure 1c,d). The position of the turn corresponds to the  
139 reduction in flexibility between residues 86-89 according to chemical shifts, but is more  
140 rigid. The same  $\beta$ -sheet-like structure is present in all five AF2 models but with variable  
141 orientation relative to the rest of the protein, perhaps indicative of dynamics. It is likely  
142 that the truth lies somewhere in between the slightly too flexible NMR structure and  
143 slightly too rigid AF2 structure. That is to say, this region in solution is dynamic and  
144 likely transitions between disorder (the NMR structure) and a loose  $\beta$ -sheet-like  
145 conformation (the AF2 model).

146 In the fourth ill-defined region (residues 144-168), the AF2 model contains an  
147  $\alpha$ -helix that is not present in the NMR structure. ANSURR shows this region is highly  
148 flexible and so does not support the existence of the helix. However,  $^{15}\text{N}$  relaxation  
149 dispersion and  $^1\text{H}$ - $^{15}\text{N}$  heteronuclear NOE data suggest this region could potentially  
150 transiently adopt secondary structure<sup>14</sup>. Given that chemical shifts represent a  
151 population-weighted average, it seems an  $\alpha$ -helix in this position would not comprise  
152 the dominant conformation in solution, as suggested previously<sup>4</sup>.

153 Overall, our analysis suggests that for T1027 the experimental NMR structure  
154 is globally more accurate than the AF2 structure. However, the picture is less clear  
155 looking at the local detail. One reason for this could be that this protein is particularly  
156 dynamic and not well described by a single structure. Our ANSURR analysis also  
157 highlights the importance of validating ill-defined regions in NMR structures. Such  
158 regions can adopt a wide range of partially ordered structures.

159



160  
161

162 **Figure 2.** ANSURR analysis of T1027. Blue lines show the rigidity as measured by  
163 RCI based on backbone chemical shifts (BMRB 36288); orange lines show the rigidity  
164 (a) of the best scoring NMR structure (model 11 from the ensemble), and (b) of the  
165 best scoring AF2 model (model 3). Red bars at the top of each figure denote  $\alpha$ -helical  
166 structure as assessed from the structure using DSSP, and blue bars denote  $\beta$ -sheet.  
167 Regions characterised as ill-defined by CYRANGE are indicated in grey.

168

### 169 **Target T1029**

170 The highest scoring CASP14 prediction for T1029 had a GDT\_TS of only 45,  
171 suggesting that it and all other predicted structures were highly inaccurate. However,  
172 our ANSURR analysis reveals that the target NMR structure is actually much less  
173 accurate than many of the predicted structures. In fact, 51% of the predicted structures  
174 have better ANSURR scores than the best scoring NMR model. During the preparation  
175 of this paper, it was confirmed that the NMR structure is inaccurate<sup>4</sup>. The NOESY peak  
176 list used to generate the original NMR structure was found to be missing many peaks  
177 present in the NOESY spectra. The NOESY peaks were carefully re-picked and used  
178 to recalculate the structure. The AF2 predictions were then used to guide refinement -  
179 referred to as “inverse structure determination” by the authors. The resulting NMR  
180 structure is very similar to the AF2 structure and has much improved ANSURR scores  
181 (green points on Fig 1). Even so, the recalculated NMR structure remained slightly  
182 less accurate than the AF2 structure. More details are presented in Supplementary  
183 Information.

184

### 185 **Comparison of all available human AF2 and NMR structures**

186 Our analysis of three examples from CASP14 suggests that structures  
187 predicted by AF2 can rival or even exceed the accuracy of NMR structures. To  
188 investigate this more broadly we extended our study to compare 904 human protein  
189 structures from the recently published AlphaFold Protein Structure Database<sup>12</sup> with  
190 their NMR structure counterparts from the PDB. ANSURR was used to validate each  
191 AF2 structure and each model in the corresponding NMR ensembles. To simplify the  
192 analysis of a large number of structures, correlation and RMSD scores generated by

193 ANSURR were summed to obtain a single accuracy score, termed ANSURR score, as  
194 described previously<sup>11</sup>. Individual correlation and RMSD scores are provided in  
195 supplementary information.

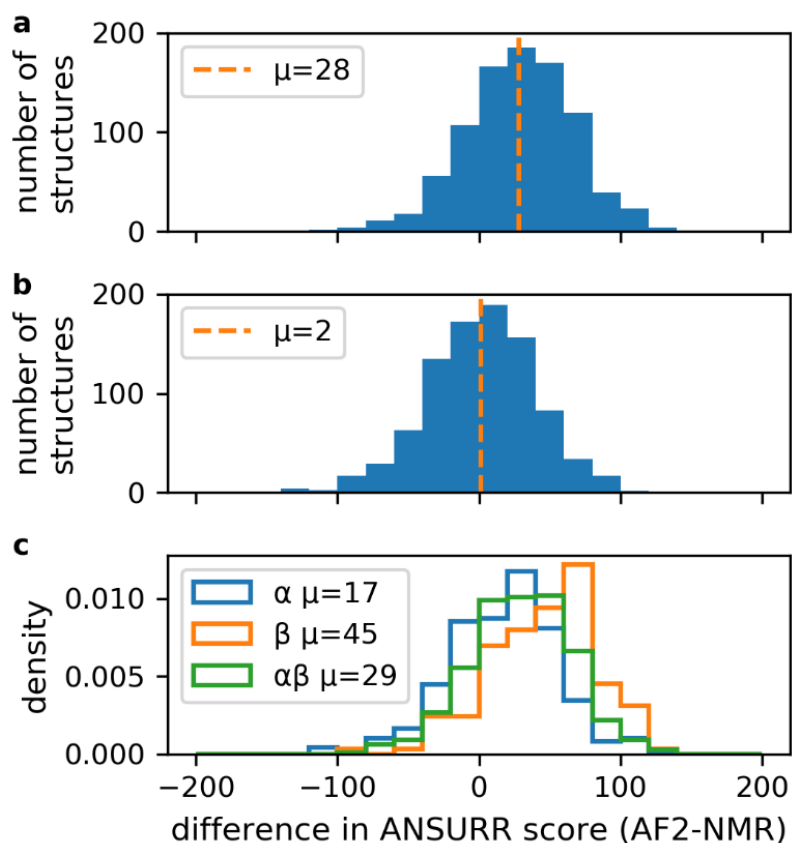
196

197 Figure 3a shows the difference in ANSURR score between the AF2 models and the  
198 models from the corresponding NMR ensembles. AF2 structures tend to be more  
199 accurate than NMR structures, with a mean difference in ANSURR score of 28. The  
200 ANSURR score is a ranked centile score on a range from 0 to 200: this difference  
201 therefore represents a significantly better performance for AF2 compared to NMR. We  
202 have previously shown<sup>11</sup> that the accuracy of the different structures within the NMR  
203 ensemble varies widely. In Figure 3b, we therefore compare the AF2 prediction to the  
204 best scoring model from the NMR ensemble. The difference in ANSURR score is now  
205 only 2, indicating a very similar overall accuracy for the two methods, though with a  
206 wide spread.

207 Fig 3c depicts the difference in ANSURR score between AF2 and NMR  
208 structures according to regular secondary structure content. We find the difference in  
209 accuracy is particularly apparent for  $\beta$ -sheet proteins (mean difference of 45) whereas  
210 the accuracy of  $\alpha$ -helical proteins is closer (mean difference of 17). The difference for  
211 proteins with mixed secondary structure content falls in between (mean difference of  
212 29). These results make sense as  $\alpha$ -helices have limited variation in local geometry  
213 and so hydrogen bonds (important for imparting rigidity) are relatively straightforward  
214 to obtain during refinement. In contrast,  $\beta$ -sheets can adopt a wider range of local  
215 geometries making it more challenging to correctly resolve hydrogen bonds. We have  
216 noted this effect before<sup>11</sup>, finding that NMR structures often lack hydrogen bonds in  $\beta$ -  
217 sheets.

218 For a new protein target, an AF2 structure can be generated by a non-expert  
219 within a few minutes, while an NMR structure generally takes months of specialist skills  
220 and equipment. A simplistic conclusion would therefore be that AF2 is quicker, cheaper  
221 and at least as accurate, and so should be the preferred method for generation of  
222 structural models. However, the reality is more nuanced, and we approached it by  
223 looking in more detail at instances where one method represents a significant  
224 improvement over the other.

225



226  
227  
228  
229  
230  
231  
232  
233  
234  
235  
236  
237  
238  
239

**Figure 3.** Frequency distribution for the difference in ANSURR score between the AF2 prediction and NMR structure, given as [AF2 score] – [NMR score] so that a positive difference indicates a better score for the AF2 prediction. Selection criteria are outlined in Methods. (a) Comparison of AF2 to the averaged ANSURR score for the NMR ensemble. Mean difference is 28. (b) Comparison of AF2 to the single best NMR structure in the ensemble (ie, the NMR structure with the best ANSURR score). Mean difference is 2. (c) Breakdown of the data in (a) by protein secondary structure classification as determined by DSSP, using proteins classified as  $\alpha$ -helical,  $\beta$ -sheet or mixed  $\alpha/\beta$ .

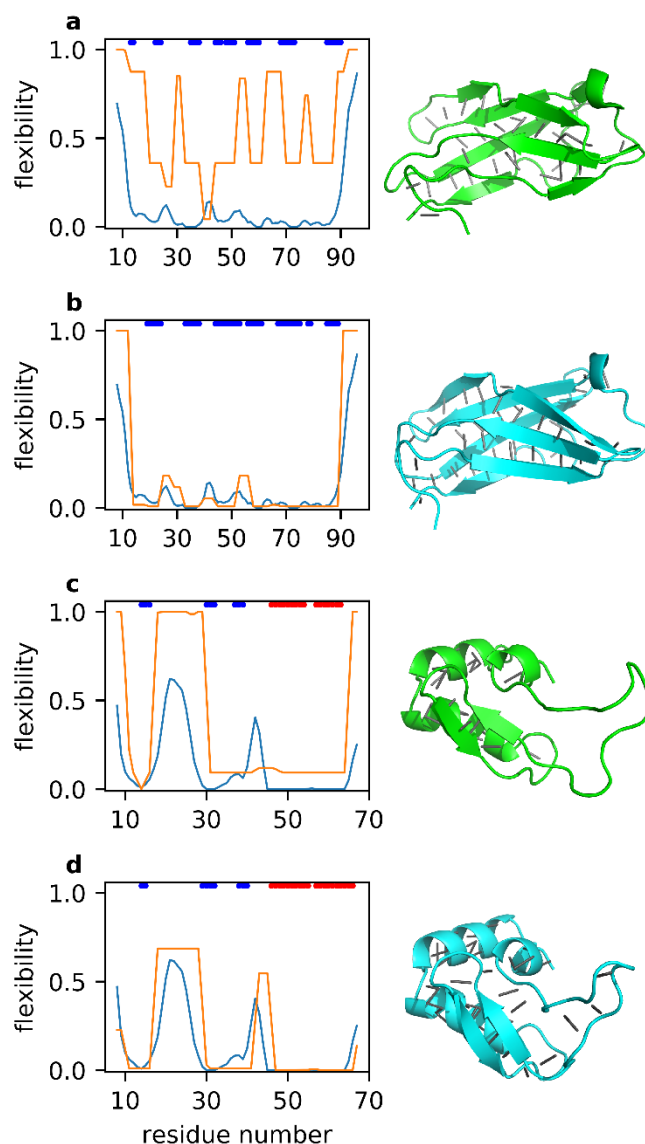
### 240 **Examples where AlphaFold structures are significantly more accurate than** 241 **NMR structures**

242 To understand why AF2 structures tend to be more accurate than NMR  
243 structures, we looked more closely at the AF2 structures that had ANSURR scores at  
244 least 50 greater than those of the NMR structures. There were 282 such structures  
245 (31% of the 904). The increased accuracy largely stemmed from AF2 models having  
246 more extensive hydrogen bond networks than NMR structures, which results in them  
247 being more rigid overall, giving them a higher ANSURR RMSD score. We have noted  
248 previously<sup>11</sup> that NMR structures tend to be too floppy, and that increasing the rigidity  
249 of the NMR structure by addition of hydrogen bonds generally improves its ANSURR  
250 score. The locations of the hydrogen bonds do of course have to be correct, and AF2  
251 provides accurate predictions of hydrogen bond locations<sup>1</sup>. Figure 4 provides two  
252 examples.

253            Figures 4a and 4b depict the ANSURR output for the 20th Filamin domain from  
254 human Filamin-B, a fairly rigid protein, while Figures 4c and 4d depict ANSURR output  
255 for a much more flexible zinc finger domain. For both proteins, the AF2 structure has  
256 greater rigidity, and matches better to the rigidity determined from experimental  
257 chemical shifts. For the Filamin domain (Figs 4a and b) the additional hydrogen bonds  
258 mainly define and extend the  $\beta$ -sheet regions better (and more correctly). The zinc  
259 finger (Figs 4c and d) has a large flexible loop between residues 16-30 which is  
260 completely lacking any backbone hydrogen bonds in the NMR structure. However, the  
261 AF2 structure contains six backbone hydrogen bonds in this region, so that the loop  
262 adopts a loose  $\beta$ -sheet-like conformation. These hydrogen bonds act to reduce the  
263 overall flexibility, and more specifically in a way that leads to better agreement with the  
264 flexibility obtained from chemical shifts, suggesting that they persist in solution. In  
265 summary, we suggest that the AF2 models tend to be better than NMR structures  
266 because they contain not just more hydrogen bonds but also correct hydrogen bonds  
267 that tend to persist in solution.  
268  
269  
270



271  
272



273  
274

275 **Figure 4.** Representative ANSURR output for two proteins where the AF2 model is  
276 more accurate than the NMR structure. Each panel shows the rigidity from chemical  
277 shifts in blue, and the structure rigidity in orange. The colored bars at the top of each  
278 plot indicate regions of regular secondary structure:  $\alpha$ -helix (red) and  $\beta$ -sheet (blue).  
279 The structures are shown beside each plot in cartoon representation, with backbone  
280 hydrogen bonds depicted as grey lines. (a) and (b): 20th Filamin domain from human  
281 Filamin-B. (a) is the NMR structure (PDB ID 2dlg, model 19) and (b) is the AF2 model  
282 (UniProt O75369). (c) and (d): the zinc finger BED domain of the zinc finger BED  
283 domain containing protein 1. (c) is the NMR structure (PDB ID 2ct5, model 3) and (d)  
284 is the AF2 model (UniProt O96006).

285  
286  
287  
288

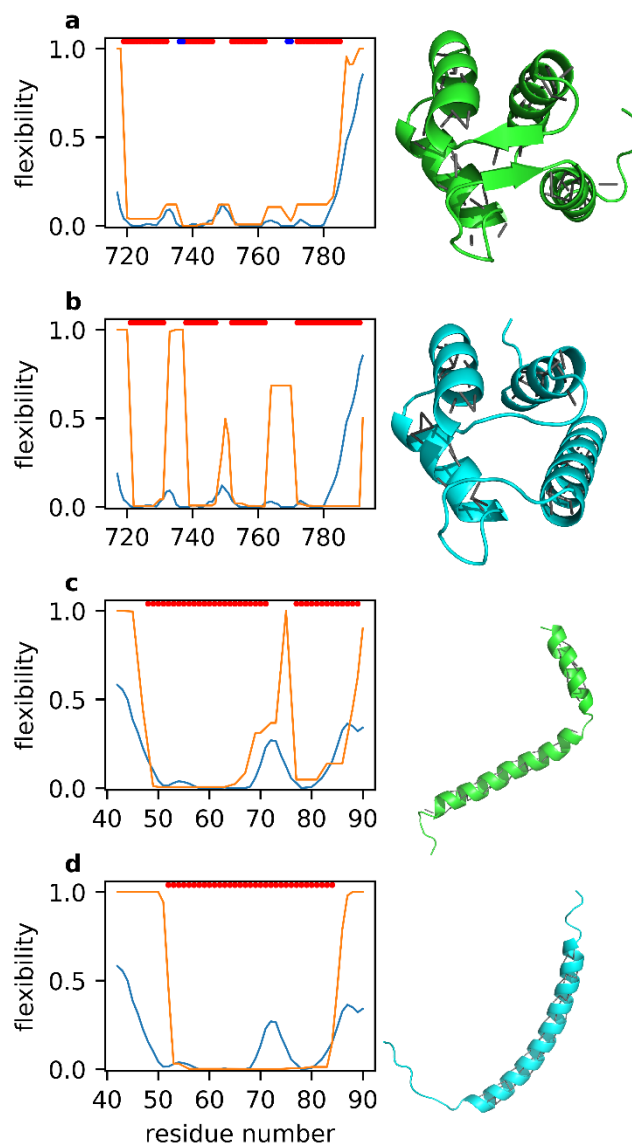
**Examples where NMR structures are significantly more accurate than AlphaFold structures**

289           There were only 25 instances (3% of the 904) where NMR structures had an  
290 ANSURR score at least 50 greater than the AF2 structure. From the ANSURR output  
291 and inspection of the structures we find that there are three main reasons as to why.

292           First, in some cases better ANSURR scores were achieved due to differences  
293 in terminal regions that likely result from NMR measurements being performed on  
294 constructs representing only part of an entire protein e.g. a single domain. The models  
295 in the AlphaFold Protein Structure Database cover the entire sequence associated  
296 with a particular UniProt accession number whereas many NMR structures only  
297 represent some portion. As a result, terminal regions in NMR structures are likely to  
298 be more disordered/flexible than they would be as part of a larger construct, which  
299 could explain differences between NMR and AF2 structures at the C-terminal end of  
300 Figs 5a,b. An example outlining this in more detail is included in SI Figure 5. It should  
301 be noted that because we use the chemical shifts associated with an NMR structure,  
302 we are biased towards favouring NMR structures. This makes the high ANSURR  
303 scores obtained by the AF2 structures even more impressive.

304           Second, some AF2 models are missing the correct regular secondary structure.  
305 An example is shown in Figs 5a,b, where the NMR structure has a short  $\beta$ -sheet region  
306 which is missing in the AF2 structure. As a result, the AF2 structure is much too flexible  
307 between residues 732-738 and 763-771. We note that AF2 produces its own  
308 confidence score called per-residue local difference distance test (pLDDT). AF2  
309 correctly indicates confidence in this particular prediction as “low” with a mean pLDDT  
310 of 66 (out of a maximum of 100, SI Figure 6a).

311           Third, some AF2 models have incorrect secondary structure. Figure 5c shows  
312 the NMR structure of a membrane-associated  $\alpha$ -helix with a break that is reflected in  
313 both the flexibility determined from chemical shifts and the computed flexibility. In  
314 contrast, the AF2 structure does not have the break, clearly in violation of the NMR  
315 data. As before, AF2 correctly indicates “low confidence” in the prediction, with a mean  
316 pLDDT of 58 and particularly low confidence in the region that should contain the break  
317 (SI Figure 6b). We speculate that AF2 will struggle to predict breaks in helices as they  
318 are less commonly observed in crystal structures (because they are difficult to  
319 crystallise or because crystallisation stabilises unbroken helices) and are therefore  
320 under-represented in the AF2 training data.



321  
322

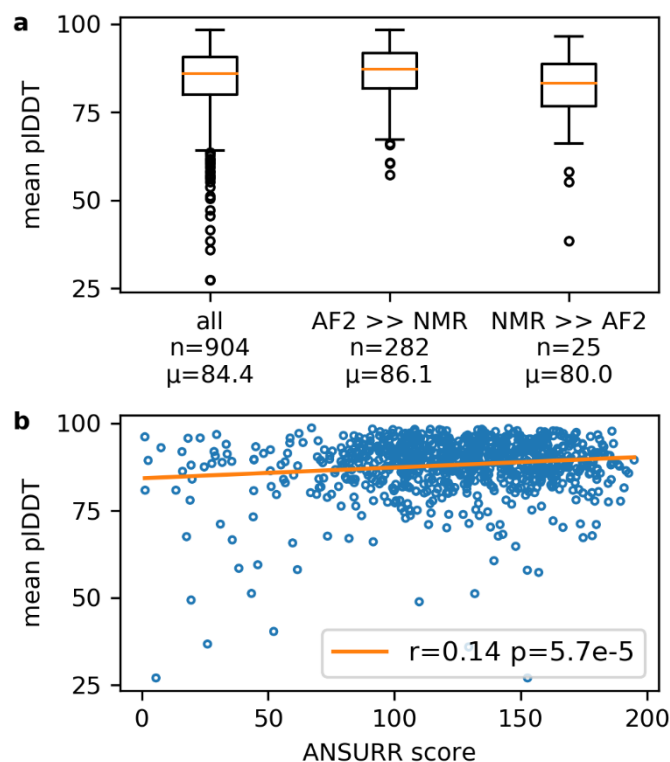
323 **Figure 5.** Representative ANSURR output for two proteins where the NMR structure  
324 is better than the AF2 model. Color scheme as for Figure 4. The structures are shown  
325 beside each plot in cartoon representation, with backbone hydrogen bonds depicted  
326 as grey lines. (a) and (b): EF-hand domain of human polycystin 2. (a) is the NMR  
327 structure (PDB ID 2y4q, model 3) and (b) is the AF2 structure (UniProt Q13563). (c)  
328 and (d): transmembrane and juxtamembrane domains of epidermal growth factor  
329 receptor in DPC micelles. (c) is the NMR structure (PDB ID 2n5s, model 2), and (d) is  
330 the AF2 structure (UniProt P00533),

331  
332

### 333 Comparison of estimated per-residue pLDDT and ANSURR scores

334 Figure 6 shows two examples where the AF2 structures are less accurate than  
335 NMR structures. In both cases, AF2 had correctly identified a low confidence in the  
336 predictions, via a low mean pLDDT. We therefore carried out an analysis to see  
337 whether mean pLDDT can be used as a measure of accuracy. Figure 6a shows that  
338 the AF2 models that have significantly better ANSURR score than the NMR structures  
339 (AF2 >> NMR) have a larger mean pLDDT, whereas the AF2 models that have

340 significantly worse ANSURRE scores have a smaller mean pLDDT. However overall  
341 there is little correlation between pLDDT and ANSURRE score (Fig 6b). In a paper  
342 accompanying the public release of AF2, it was demonstrated that regions with low  
343 pLDDT tend to be disordered, to the extent that pLDDT can be used as highly  
344 competitive disorder predictor<sup>15,16</sup>. Hence, AF2 may assign low confidence to a  
345 disordered region which ANSURRE highlights as accurate because it correctly lacks  
346 structure (see Figure 4c,d as an example of how ANSURRE can distinguish between  
347 regions of high flexibility and complete disorder).  
348  
349  
350



351  
352 **Figure 6.** A comparison of pLDDT scores to ANSURRE scores. (a) The mean pLDDT  
353 score averaged over all amino acids for each AF2 model. Statistics are shown for all  
354 AF2 models in the test set, and separately for the 282 structures in which the AF2  
355 structure is significantly better than the NMR structure, and for the 25 structures in  
356 which the NMR structure is significantly better than the AF2 structure. The mean  
357 pLDDT score is shown below each box. (b) Correlation plot for mean pLDDT scores  
358 vs ANSURRE scores for each AF2 model in the test set. The orange line is the line of  
359 best fit. Pearson's r and the corresponding two-tailed p value are given in the legend.

## 360 361 Discussion

362 It is already clear that the availability, simplicity and remarkable accuracy of AF2  
363 will make it invaluable for modelling protein structures, for example for the design of  
364 drugs that work by binding to the protein. However, this is only true as long as the AF2  
365 models are good models for the structure of the protein in solution. The studies  
366 presented here compare AF2 models to solution chemical shifts, and provide  
367 convincing evidence for the accuracy of AF2 models as solution structures, confirming  
368 earlier reports<sup>17,18</sup>. Nevertheless, there are rare occasions where the AF2 models are

369 incorrect, likely because they do not adequately represent the dynamics of proteins in  
370 solution. Can NMR be used to identify and correct such errors?

371 Two reviews comparing NMR and crystal structures<sup>6,7</sup> have concluded that  
372 NMR structures have the same fold as corresponding crystal structures, but are on  
373 average of lower quality. Our own analysis using ANSURRE<sup>10,11</sup> reached the same  
374 conclusion. An interesting point made by Andrec, et al.<sup>7</sup> is that the precision of the  
375 NMR ensemble is tighter than the average distance between the NMR ensemble and  
376 the crystal structure: that is, that the most obvious measure of the “error” of the NMR  
377 structures is misleadingly small - not only are NMR structures of low quality but the  
378 error attached to them is unreliable. More recent analyses have reached similar though  
379 slightly more optimistic conclusions: thus, Schneider, et al.<sup>19</sup> showed that NMR  
380 structures can be useful templates for structural models; Abaturov and Nosova<sup>20</sup>  
381 showed that structural differences are minimised by collecting more NMR data; Li and  
382 Brüsweiler<sup>21</sup> showed that molecular dynamics optimisation of NMR structures can  
383 make them much more comparable to crystal structures; Everett, et al.<sup>22</sup> revisited the  
384 analysis of Andrec, et al.<sup>7</sup>, and concluded that agreement between NMR and crystal  
385 structures is improved by using modern NMR methods; and Faraggi, et al.<sup>23</sup> concluded  
386 that much of the difference may reflect genuinely increased mobility in solution. We  
387 have shown that although NMR structures are significantly too floppy by comparison  
388 to chemical shift data, crystal structures are too rigid. Indeed, numerous studies have  
389 shown that NMR structures can represent the dynamic nature of protein structures in  
390 solution better than crystal structures: for example<sup>24,25</sup>. These studies are of relevance  
391 to the current work, because AF2 predictions are trained on crystal structures. Thus,  
392 if NMR can be used to “correct” crystal structures to produce a more correct dynamic  
393 solution structure, it can clearly do the same also for AF2 structures.

394 Most AF2 structures are at least as accurate as NMR ensembles. Calculation  
395 of an AF2 prediction takes minutes and can be done with minimal training. By contrast,  
396 the calculation of an NMR structure usually takes months, and requires expensive  
397 equipment and a trained operator. It is impractical to calculate an NMR structure for  
398 every target. However, the backbone NMR assignment of small to medium sized  
399 proteins can be done almost automatically<sup>26,27</sup>, and permits the application of  
400 ANSURRE. On the basis of the results presented here, we therefore propose that it  
401 would make sense to test the accuracy of AF2 models by carrying out semi-automated  
402 backbone assignment, followed by ANSURRE. A model validated by ANSURRE can be  
403 accepted as an accurate solution model (with no need for further NMR structure  
404 calculation), while models that have clear local violations need revision and would be  
405 good targets for NMR-based structure refinement of the AF2 model. Figure 7ab  
406 provides a good example of how this could be done. ANSURRE shows that the AF2  
407 model for human polycystin 2 (UniProt Q13563) is inaccurate in that it is missing a  
408 short antiparallel  $\beta$ -sheet present in solution. It would be straightforward to calculate a  
409 more accurate structure by starting from the AF2 model and adding additional  
410 restraints to resolve the  $\beta$ -sheet.

411 It may be argued that such a procedure biases the resulting NMR structure by  
412 imposing interatomic interactions present in the AF2 starting model. However, bias of  
413 this type is imposed on every NMR structure calculation by the use of knowledge-  
414 based restraints. The use of an AF2 model is just a more sophisticated version of a  
415 knowledge-based restraint and should be welcomed.

416 A complementary approach would be to produce a modified version of AF2  
417 trained to generate more accurate solution structures, by “learning” the locations of  
418 dynamic structure. Such an approach would be enormously powerful, but would of

419 course require the generation of appropriate training sets. The most obvious way of  
420 providing suitable training sets is via NMR chemical shifts, which carry all the  
421 information needed to characterise local dynamic regions<sup>28,29</sup> and are often available  
422 from the Biological Magnetic Resonance Data Bank (BMRB)<sup>30</sup>. Alternatively, training  
423 data for solution structure and dynamics could be generated from molecular  
424 simulations<sup>31</sup> or deep learning methods<sup>32</sup>.

425 Finally, we note that most structure calculations and structure predictions  
426 assume that the structure can be represented by a single structure. In general this  
427 seems to be true, but some of the examples discussed here suggest some element of  
428 heterogeneity, even if only in the form of folded and unfolded local structure in  
429 equilibrium. Such heterogeneity is potentially of great importance for both function and  
430 inhibition of function, and the results presented here suggest that a combination of  
431 AF2 and ANSURRE would be one way to identify and characterise such equilibria.

432

433

## 434 **Methods**

435

### 436 **A set of comparable NMR and AlphaFold structures**

437 Each structure in the AlphaFold Protein Structure Database<sup>12</sup> is indexed by a  
438 UniProt accession number. We used the Structure Integration with Function,  
439 Taxonomy and Sequence (SIFTS) resource<sup>33</sup> to map the UniProt accession number  
440 of each human protein in the AlphaFold Protein Structure database to NMR structures  
441 in PDB<sup>34</sup>. Specifically, we used the uniprot\_segments\_observed.tsv SIFTS file to  
442 identify overlapping regions between the two types of structures and extracted these  
443 regions from the structure files using an in-house program. AF2 structures do not  
444 contain hydrogen atoms, so we added them using the program REDUCE v3.23<sup>35</sup>. We  
445 applied the following criteria to filter out NMR structures which could complicate our  
446 comparison. NMR structures needed to a) comprise only a single chain, b) have a set  
447 of backbone chemical shifts in the BMRB with at least 75% completeness, to ensure  
448 the reliability of ANSURRE, and c) have at least 20 amino acid residues. The final set  
449 consisted of 904 AlphaFold/NMR structure pairs. A summary listing UniProt accession  
450 numbers and PDB IDs of the mapped AF2/NMR structures and corresponding residue  
451 ranges is provided in a supplementary text file (comparable\_af2\_nmr\_structures.txt).

452

### 453 **ANSURRE calculations**

454 All ANSURRE calculations were performed with ANSURRE v1.1.0 (DOI  
455 10.5281/zenodo.4984229) with the following options: re-reference chemical shifts  
456 using PANA, include non-standard residues when computing flexibility, do not include  
457 ligands when computing flexibility. NMR structures contain multiple models (typically  
458 20) and so we computed ANSURRE scores for all models and averaged them to obtain  
459 a single ANSURRE score for each PDB entry. Each AF2 structure could be mapped to  
460 multiple PDB entries. In this case we computed the average ANSURRE score of the  
461 PDB entries and compared this to the average ANSURRE score computed for regions  
462 taken from the AF2 structure which overlapped with the PDB entries. For example,  
463 AF2 structure O00206 was mapped to two PDB entries (5NAM and 5NAO), so we  
464 compared the average ANSURRE score for the two PDB entries with the average  
465 ANSURRE score for models comprising residues 623-670 and residues 623-657 from  
466 the AF2 structure. Individual ANSURRE scores for all structures validated in this work  
467 are provided as supplementary text files (AF2 – af2\_ansurr\_scores.txt, NMR –  
468 nmr\_ansurr\_scores.txt). We chose not to include ligands when computing flexibility as

469 they are not present in AF2 structures. We therefore felt that removing any ligands  
470 from NMR structures was the fairest comparison. We showed previously<sup>11</sup> that ligands  
471 can cause changes in computed flexibility, but that the overall effect on ANSURR score  
472 is small: including ligands to compute flexibility for a set of 162 NMR ensembles led to  
473 a mean change in ANSURR score of only 1. Secondary structure was classified using  
474 DSSP v2.0.4<sup>36</sup>.

475

476 **Data availability.** Source data are listed in Supplementary Information and are from  
477 publicly available databases: specifically, the Protein Data Bank ([www.rcsb.org](http://www.rcsb.org)),  
478 Biological Magnetic Resonance Bank (BMRB: [www.bmr.io](http://www.bmr.io)) and the AlphaFold Protein  
479 Structure Database (<https://alphafold.ebi.ac.uk>). The accession codes of PDB and  
480 BMRB entries used in this study are listed in the file `comparable_af2_nmr_structures`.  
481 Data supporting the findings of this work are available within the paper and its  
482 Supplementary Information. The datasets generated and analysed during the current  
483 study are available from the authors upon request.

484

## 485 References

- 486 1. Jumper, J. et al. Highly accurate protein structure prediction with AlphaFold.  
487 *Nature* **596**, 583-589 (2021).
- 488 2. Pereira, J. et al. High-accuracy protein structure prediction in CASP14.  
489 *Proteins-Structure Function and Bioinformatics* **89**, 1687-1699 (2021).
- 490 3. Alexander, L.T. et al. Target highlights in CASP14: Analysis of models by  
491 structure providers. *Proteins-Structure Function and Bioinformatics* **89**, 1647-  
492 1672 (2021).
- 493 4. Huang, Y. et al. Assessment of prediction methods for protein structures  
494 determined by NMR in CASP14: Impact of AlphaFold2. *Proteins Struct. Funct.*  
495 *Bioinf.* **89**, 1959-1976 (2021).
- 496 5. Williamson, M.P., Havel, T.F. & Wüthrich, K. Solution conformation of  
497 proteinase inhibitor IIA from bull seminal plasma by <sup>1</sup>H nuclear magnetic  
498 resonance and distance geometry. *J. Mol. Biol.* **182**, 295-315 (1985).
- 499 6. Billeter, M. Comparison of protein structures determined by NMR in solution  
500 and by X-ray diffraction in single crystals. *Quarterly Reviews of Biophysics* **25**,  
501 325-377 (1992).
- 502 7. Andrec, M. et al. A large data set comparison of protein structures determined  
503 by crystallography and NMR: Statistical test for structural differences and the  
504 effect of crystal packing. *Proteins: Struct. Funct. Bioinf.* **69**, 449-465 (2007).
- 505 8.
- 506 9. Berjanskii, M.V. & Wishart, D.S. Application of the random coil index to  
507 studying protein flexibility. *Journal of Biomolecular NMR* **40**, 31-48 (2008).
- 508 10. Fowler, N.J., Sljoka, A. & Williamson, M.P. A method for validating the  
509 accuracy of NMR protein structures. *Nature Communications* **11**, 6321 (2020).
- 510 11. Fowler, N.J., Sljoka, A. & Williamson, M.P. The accuracy of NMR protein  
511 structures in the Protein Data Bank. *Structure* **29**, 1430-1439 (2021).
- 512 12. Varadi, M. et al. AlphaFold Protein Structure Database: massively expanding  
513 the structural coverage of protein-sequence space with high-accuracy models.  
514 *Nucleic acids research* **50**, D439-D444 (2022).
- 515 13. Kirchner, D.K. & Güntert, P. Objective identification of residue ranges for the  
516 superposition of protein structures. *Bmc Bioinformatics* **12**, 170 (2011).

- 517 14. Wu, N. et al. Solution structure of *Gaussia* Luciferase with five disulfide bonds  
518 and identification of a putative coelenterazine binding cavity by heteronuclear  
519 NMR. *Scientific Reports* **10**, 20069 (2020).
- 520 15. Tunyasuvunakool, K. et al. Highly accurate protein structure prediction for the  
521 human proteome. *Nature* **596**, 590-596 (2021).
- 522 16. Ruff, K.M. & Pappu, R.V. AlphaFold and implications for intrinsically  
523 disordered proteins. *Journal of Molecular Biology* **433**, 167208 (2021).
- 524 17. Robertson, A.J., Courtney, J.M., Shen, Y., Ying, J. & Bax, A. Concordance of  
525 X-ray and AlphaFold2 models of SARS-CoV-2 main protease with residual  
526 dipolar couplings measured in solution. *Journal of the American Chemical  
527 Society* **143**, 19306-19310 (2021).
- 528 18. Zweckstetter, M. NMR hawk-eyed view of AlphaFold2 structures. *Protein  
529 Science* **30**, 2333-2337 (2021).
- 530 19. Schneider, M., Fu, X. & Keating, A.E. X-ray vs. NMR structures as templates  
531 for computational protein design. *Proteins-Structure Function and  
532 Bioinformatics* **77**, 97-110 (2009).
- 533 20. Abaturov, L.V. & Nosova, N.G. Crystallographic and NMR spectroscopic  
534 protein structures: Interresidue contacts. *Molecular Biology* **46**, 287-303  
535 (2012).
- 536 21. Li, D.-W. & Brüschweiler, R. Protocol to make protein NMR structures  
537 amenable to stable long time scale molecular dynamics simulations. *Journal  
538 of Chemical Theory and Computation* **10**, 1781-1787 (2014).
- 539 22. Everett, J.K. et al. A community resource of experimental data for NMR/X-ray  
540 crystal structure pairs. *Protein Science* **25**, 30-45 (2016).
- 541 23. Faraggi, E., Dunker, A.K., Sussman, J.L. & Kloczkowski, A. Comparing NMR  
542 and X-ray protein structure: Lindemann-like parameters and NMR disorder.  
543 *Journal of Biomolecular Structure & Dynamics* **36**, 2331-2341 (2018).
- 544 24. Tomlinson, J.H., Ullah, S., Hansen, P.E. & Williamson, M.P. Characterization  
545 of salt bridges to lysines in the protein G B1 domain. *J. Am. Chem. Soc.* **131**,  
546 4674-4684 (2009).
- 547 25. Ikura, M. et al. Secondary structure and side-chain <sup>1</sup>H and <sup>13</sup>C resonance  
548 assignments of calmodulin in solution by heteronuclear multidimensional NMR  
549 spectroscopy. *Biochemistry* **30**, 9216-9228 (1991).
- 550 26. Würz, J.M., Kazemi, S., Schmidt, E., Bagaria, A. & Güntert, P. NMR-based  
551 automated protein structure determination. *Archives of Biochemistry and  
552 Biophysics* **628**, 24-32 (2017).
- 553 27. Williamson, M.P. & Craven, C.J. Automated protein structure calculation from  
554 NMR data. *J. Biomol. NMR* **43**, 131-143 (2009).
- 555 28. Dass, R., Mulder, F.A.A. & Nielsen, J.T. ODiNPred: comprehensive prediction  
556 of protein order and disorder. *Scientific Reports* **10**, 14780 (2020).
- 557 29. Kagami, L.P. et al. b2bTools: online predictions for protein biophysical features  
558 and their conservation. *Nucleic Acids Research* **49**, W52-W59 (2021).
- 559 30. Ulrich, E.L. et al. BioMagResBank. *Nucleic Acids Res.* **36**, D402-D408 (2008).
- 560 31. Ramaswamy, V.K., Musson, S.C., Willcocks, C.G. & Degiacomi, M.T. Deep  
561 learning protein conformational space with convolutions and latent  
562 interpolations. *Physical Review X* **11**, 011052 (2021).
- 563 32. Noé, F., Olsson, S., Köhler, J. & Wu, H. Boltzmann generators: Sampling  
564 equilibrium states of many-body systems with deep learning. *Science* **365**,  
565 eaaw1147 (2019).



- 566 33. Dana, J.M. et al. SIFTS: updated Structure Integration with Function,  
567 Taxonomy and Sequences resource allows 40-fold increase in coverage of  
568 structure-based annotations for proteins. *Nucleic Acids Research* **47**, D482-  
569 D489 (2019).
- 570 34. Burley, S.K. et al. Protein Data Bank: the single global archive for 3D  
571 macromolecular structure data. *Nucleic Acids Research* **47**, D520-D528  
572 (2019).
- 573 35. Word, J.M., Lovell, S.C., Richardson, J.S. & Richardson, D.C. Asparagine and  
574 glutamine: Using hydrogen atom contacts in the choice of side-chain amide  
575 orientation. *Journal of Molecular Biology* **285**, 1735-1747 (1999).
- 576 36. Touw, W.G. et al. A series of PDB-related databanks for everyday needs.  
577 *Nucleic Acids Research* **43**, D364-D368 (2015).
- 578

579 **Acknowledgements.** We thank the Biotechnology and Biological Science Research  
580 Council (BBSRC) for funding to N. J. F. (BB/P020038/1).

581

582 **Author contributions.** Both authors conceived the study and wrote the manuscript.  
583 N. J. F. wrote the code and did the analysis.

584

585 **Competing interests.** The authors declare no competing interests.

586